ARTS ET MÉTIERS ParisTech Lille

24th International Congress of Theorical and Applied Mechanics

HARDENING SOFTENING BEHAVIOR OF ANTIRESONANCE FOR NON LINEAR TORSIONAL VIBRATION ABSORBERS

[1,2]Alexandre Renault, [1]Olivier Thomas

[1]Arts et Métiers ParisTech, LSIS UMR CNRS 7296, 8 bd. Louis XIV 59000 Lille, France.

11th October 2016

Laboratoire des Sciences de l' Information et des Systèmes

Motivation

- Common thermal engines produce a highly acyclic torque

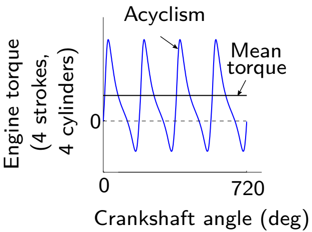

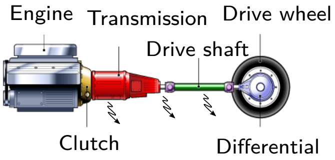

Motivation

- Common thermal engines produce a highly acyclic torque

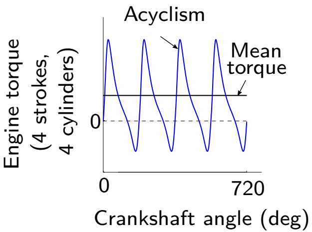

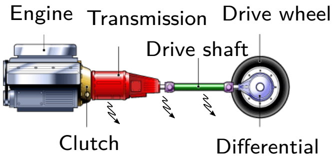

- Source of noise, wear, passenger discomfort ...

Motivation

- Common thermal engines produce a highly acyclic torque

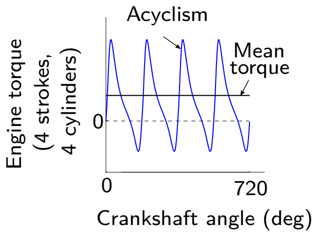

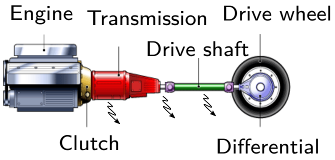

- Source of noise, wear, passenger discomfort ...

- The torque irregularities frequency ω_e is at an order n_e of the mean engine speed of rotation Ω

$$T(t) = T_0 \cos \omega_e t \;, \quad \omega_e = n_e \Omega$$

- The firing order, n_e, is the number of explosion per crankshaft revolution
  - 4 strokes, 3 cylinders $\rightarrow n_e = \frac{3}{2}$
  - 4 strokes, 4 cylinders $\rightarrow n_e = 2$

Objective

- **Objective** : Absorb acyclisms ahead of the drive line

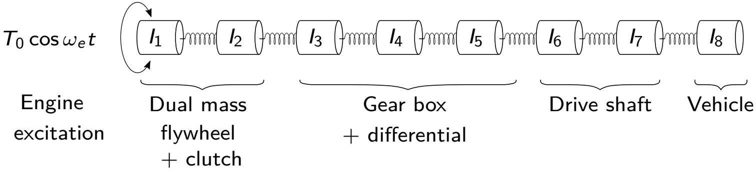

$\omega_e = n_e \Omega$

$\Omega \rightarrow$ mean engine speed of rotation

Objective

- **Objective** : Absorb acyclisms ahead of the drive line
  - Using a passive Torsional Vibration Absorber (TVA)

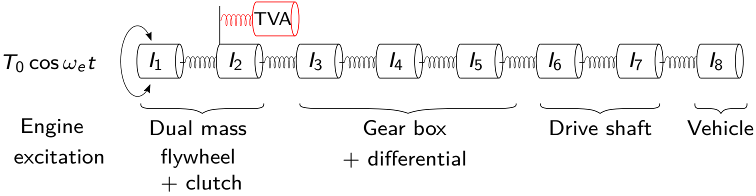

$\omega_e = n_e \Omega$

$\Omega \rightarrow$ mean engine speed of rotation

Objective

- **Objective** : Absorb acyclisms ahead of the drive line
  - Using a passive Torsional Vibration Absorber (TVA)

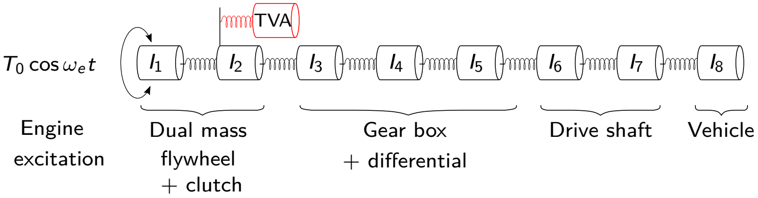

$\omega_e = n_e \Omega$

$\Omega \rightarrow$ mean engine speed of rotation

- The excitation frequency ω_e linearly depends on Ω
  - Classical tuned mass dampers operate at a given frequency
  - Pendular absorbers operate for all Ω

Pendular oscillators

Pendulum in the gravitational acceleration field

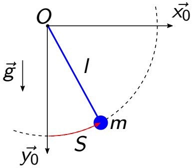

$$\ddot{S} + \omega_{0g}^2 \sin S = 0, \quad \omega_{0g}^2 = \frac{g}{l}$$

Pendular oscillators

Pendulum in the gravitational acceleration field

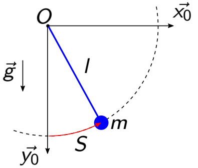

$$\ddot{S} + \omega_{0g}^2 \sin S = 0, \quad \omega_{0g}^2 = \frac{g}{l}$$

Pendulum in the centrifugal acceleration field (gravity neglected)

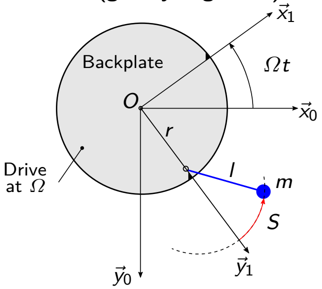

$$\ddot{S} + \omega_{0p}^2 \sin S = 0, \quad \omega_{0p}^2 = \frac{r\Omega^2}{l}$$

- The gravitational acceleration constant g is replaced by the centrifugal acceleration $r\Omega^2$

Pendular oscillators

Pendulum in the gravitational acceleration field

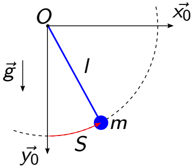

Pendulum in the centrifugal acceleration field (gravity neglected)

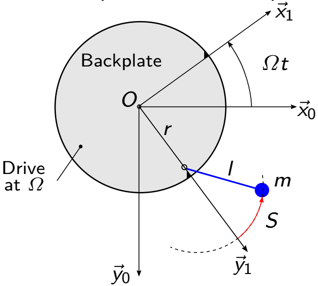

$$\ddot{S} + \omega_{0g}^2 \sin S = 0, \quad \omega_{0g}^2 = \frac{g}{l}$$

$$\ddot{S} + \omega_{0p}^2 \sin S = 0, \quad \omega_{0p}^2 = \frac{r\Omega^2}{l}$$

- The gravitational acceleration constant g is replaced by the centrifugal acceleration $r\Omega^2$
- The natural frequency is proportional to the mean engine speed of rotation Ω

$$\omega_{0p} = \Omega\sqrt{\frac{r}{l}} = \Omega n_p, \quad n_p = \sqrt{\frac{r}{l}}$$

Linear response of pendular absorbers

- The backplate is now free to rotate in the rotating frame $(\vec{x}_\Omega, \vec{y}_\Omega)$ and subjected to an external oscillating torque $T(t) = T_0 \cos n\Omega t$

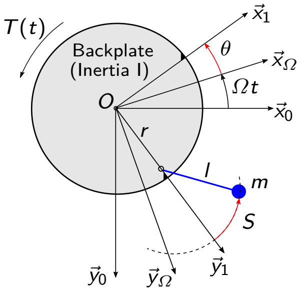

Linear response of pendular absorbers

- The backplate is now free to rotate in the rotating frame $(\vec{x}_\Omega, \vec{y}_\Omega)$ and subjected to an external oscillating torque $T(t) = T_0 \cos n\Omega t$

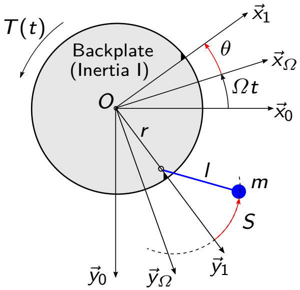

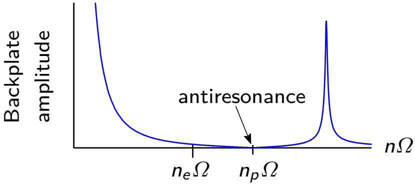

- An antiresonance occurs on the frequency response of the backplate at $n = n_p$

Linear response of pendular absorbers

- The backplate is now free to rotate in the rotating frame $(\vec{x}_\Omega, \vec{y}_\Omega)$ and subjected to an external oscillating torque $T(t) = T_0 \cos n\Omega t$

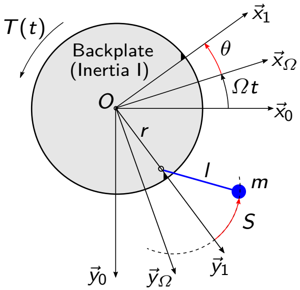

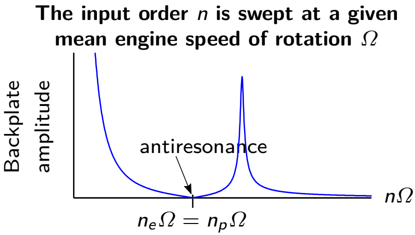

- An antiresonance occurs on the frequency response of the backplate at $n = n_p$
- The geometric parameters r and l allow to tune the absorber on the desired engine order n_e :

$$n_p = n_e, \quad n_p = \sqrt{\frac{r}{l}}$$

Particular paths

Circular pendular oscillators are non linear

$$\ddot{S} + \omega_0^2 \sin S = f \cos \omega t$$

- The resonance frequency decreases as the amplitude of oscillation increases (softening behavior)
- The response exhibits hysteretic jumps

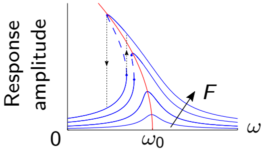

Particular paths

Circular pendular oscillators are non linear

$$\ddot{S} + \omega_0^2 \sin S = f \cos \omega t$$

- The resonance frequency decreases as the amplitude of oscillation increases (softening behavior)
- The response exhibits hysteretic jumps

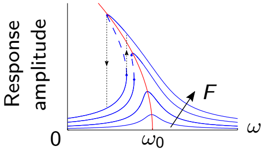

Tautochronic paths exist for which pendular oscillators behave like linear oscillators.

- In the gravitational acceleration field
  - Cycloidal path (Huygens pendulum) [Huygens 1656]
- In a constant centrifugal acceleration field
  - Epiycloidal path [Denman 1992]

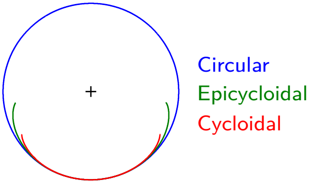

State of the art

- **Main inventors**
  - 1937, Sarazin, [US Patent 2,079,226]
  - 1938, Chilton, [US Patent 2,112,984]

State of the art

- **Main inventors**
  - 1937, Sarazin, [US Patent 2,079,226]
  - 1938, Chilton, [US Patent 2,112,984]

- **Main applications**
  - Aicraft engines, since WWII
  - Experimental automotive engines, in the 80s (US), [Shaw, Borowski, Denman, Hanisko]
  - Real interest from automotive manufacturers, since 2000

State of the art

- **Main inventors**
  - 1937, Sarazin, [US Patent 2,079,226]
  - 1938, Chilton, [US Patent 2,112,984]
- **Main applications**
  - Aicraft engines, since WWII
  - Experimental automotive engines, in the 80s (US), [Shaw, Borowski, Denman, Hanisko]
  - Real interest from automotive manufacturers, since 2000
- **Design and past work** based on : perturbation methods, time integration and experiments
  - Tautochronic vibration absorbers, [Denman 1991], [Shaw 2006 2010]
  - Dynamic response of multiple vibration absorbers, [Chao 1997 2000], [Lee 1997], [Olson 2010]
  - Stability of the dynamic response, [Chao 1997], [Shi 2012]
  - Transient dynamic response, [Monroe 2013]
  - ...

Analysis

- Pendular absorbers exhibit strong non-linearities
- We need efficient and "exact" analyse method to capture the physical behavior at large amplitude of motion
  - Low engine speed of rotation $\rightarrow$ large amplitude of oscillation

Analysis

- Pendular absorbers exhibit strong non-linearities
- We need efficient and "exact" analyse method to capture the physical behavior at large amplitude of motion
  - Low engine speed of rotation $\rightarrow$ large amplitude of oscillation
- **Pertubation methods**
  - Analytical approaches
  - Powerfull for parametric studies
  - Inappropriate for very large amplitudes

Analysis

- Pendular absorbers exhibit strong non-linearities
- We need efficient and "exact" analyse method to capture the physical behavior at large amplitude of motion
    - Low engine speed of rotation $\rightarrow$ large amplitude of oscillation
- **Pertubation methods**
    - Analytical approaches
    - Powerfull for parametric studies
    - Inappropriate for very large amplitudes
- **Numerical time integration methods**
    - Easy to implement and present in many commercial softwares
    - Require extensive computational time in case of long transient
    - No informations about unstable responses

Analysis

- Pendular absorbers exhibit strong non-linearities
- We need efficient and "exact" analyse method to capture the physical behavior at large amplitude of motion
  - Low engine speed of rotation $\rightarrow$ large amplitude of oscillation
- **Pertubation methods**
  - Analytical approaches
  - Powerfull for parametric studies
  - Inappropriate for very large amplitudes
- **Numerical time integration methods**
  - Easy to implement and present in many commercial softwares
  - Require extensive computational time in case of long transient
  - No informations about unstable responses
- **Continuation methods**
  - No transient, direct computation of the steady state
  - Give informations about unstable responses

Analysis

- Pendular absorbers exhibit strong non-linearities
- We need efficient and "exact" analyse method to capture the physical behavior at large amplitude of motion
  - Low engine speed of rotation → large amplitude of oscillation

- **Pertubation methods**
  - Analytical approaches
  - Powerfull for parametric studies
  - Inappropriate for very large amplitudes

- **Numerical time integration methods**
  - Easy to implement and present in many commercial softwares
  - Require extensive computational time in case of long transient
  - No informations about unstable responses

- **Continuation methods**
  - No transient, direct computation of the steady state
  - Give informations about unstable responses

- **Today**
  - Continuation of periodic solutions
  - The Harmonic Balance Method (HBM) [Nayfeh & Mook 1979]
  - The Asymptotic Numerical Method (ANM) [Potier-Ferry, Cochelin *et al.*, 1990-]

Model

- The investigated system is composed of 2 components
  - A backplate free in the rotating frame $(\vec{x}_\Omega, \vec{y}_\Omega)$
  - A point mass pendulum moving freely on a particular path on the backplate

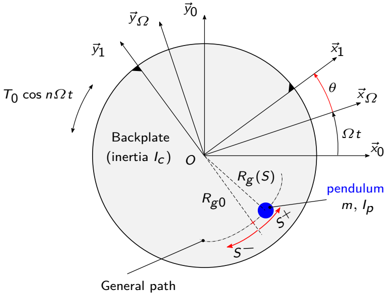

Model

- The investigated system is composed of 2 components
  - A backplate free in the rotating frame $(\vec{x}_\Omega, \vec{y}_\Omega)$
  - A point mass pendulum moving freely on a particular path on the backplate
- θ is the rotation angle of the backplate relative to the rotating frame
- S is the displacement of the pendulum along the path

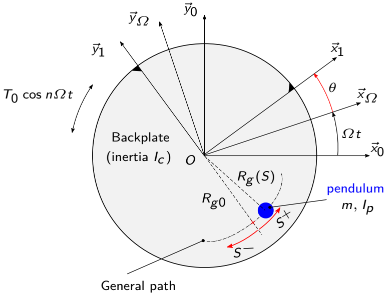

Model

- The investigated system is composed of 2 components
  - A backplate free in the rotating frame $(\vec{x}_\Omega, \vec{y}_\Omega)$
  - A point mass pendulum moving freely on a particular path on the backplate
- θ is the rotation angle of the backplate relative to the rotating frame
- S is the displacement of the pendulum along the path
- The path shape is specified by the function $X(S) = R_g^2(S)$
  - R_g is the distance from the pendulum to the point O

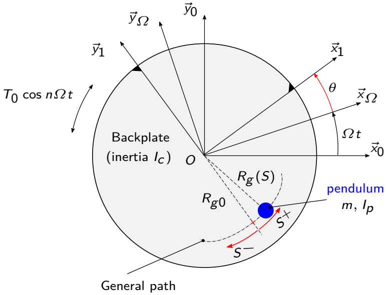

- Epicycloidal path :

$$X(S) = R_{g0}^2 - n_p^2 S^2$$

Governing equations

$$\begin{cases} \left(1 + \mu X(S)\right)\ddot{\theta} + \mu G(S)\ddot{S} + \mu\left(\dfrac{dX(S)}{dS}\dot{S}\left(\dfrac{1}{ne} + \dot{\theta}\right) + \dfrac{dG(S)}{dS}\dot{S}^2\right) + 2\xi_c\dot{\theta} = T_a \cos\dfrac{n}{n_e}\bar{t} \\ G(S)\ddot{\theta} + \ddot{S} - \dfrac{1}{2}\dfrac{dX(S)}{dS}\left(\dfrac{1}{ne} + \dot{\theta}\right)^2 + 2\xi_p\dot{S} = 0 \end{cases}$$

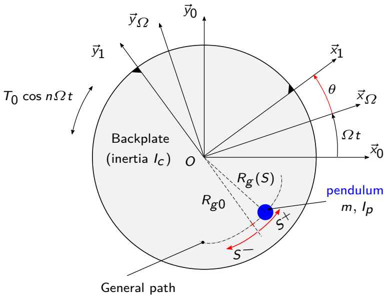

- Path geometry
  - $X = R_g^2(S)$, $G^2 = X(S) - \frac{1}{4}\left(\frac{dX(S)}{dS}\right)^2$
- Inertia ratio
  - $\mu = \frac{mR_{g0}^2}{J}$, $J = I_c + I_p$
- Damping ratios
  - $\xi_c = \frac{Cc}{2Jn_e\Omega}$, $\xi_p = \frac{Cp}{2mn_e\Omega}$
- External torque
  - $T_a = \frac{T_0}{Jn_e^2\Omega^2}$
- Rescaled time
  - $\bar{t} = n_e\Omega t$

Governing equations

$$\begin{cases} \left(1 + \mu X(S)\right)\ddot{\theta} + \mu G(S)\ddot{S} + \mu\left(\frac{dX(S)}{dS}\dot{S}\left(\frac{1}{ne}+\dot{\theta}\right) + \frac{dG(S)}{dS}\dot{S}^2\right) + 2\xi_c\dot{\theta} = T_a\cos\frac{n}{n_e}\bar{t} \\ G(S)\ddot{\theta} + \ddot{S} - \frac{1}{2}\frac{dX(S)}{dS}\left(\frac{1}{ne}+\dot{\theta}\right)^2 + 2\xi_p\dot{S} = 0 \end{cases}$$

- Geometric coupling (large rotation)
- Inertial coupling

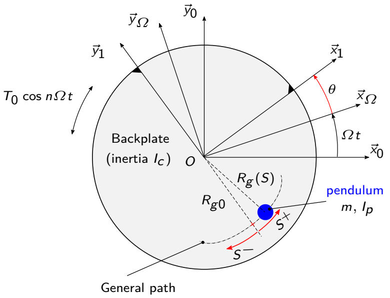

- Path geometry
  - $X = R_g^2(S)$, $G^2 = X(S) - \frac{1}{4}\left(\frac{dX(S)}{dS}\right)^2$
- Inertia ratio
  - $\mu = \frac{mR_{g0}^2}{J}$, $J = I_c + I_p$
- Damping ratios
  - $\xi_c = \frac{Cc}{2Jn_e\Omega}$, $\xi_p = \frac{Cp}{2mn_e\Omega}$
- External torque
  - $T_a = \frac{T_0}{Jn_e^2\Omega^2}$
- Rescaled time
  - $\bar{t} = n_e\Omega t$

Frequency approach

- Governing equations can be written in the following form

$$\boldsymbol{M}(\boldsymbol{x})\ddot{\boldsymbol{x}} + \boldsymbol{f_{in}}(\boldsymbol{x}, \dot{\boldsymbol{x}}) + \boldsymbol{C}\dot{\boldsymbol{x}} + \boldsymbol{f_{int}}(\boldsymbol{x}) = \boldsymbol{T}\cos(\omega t)$$

Frequency approach

- Governing equations can be written in the following form

$$\boldsymbol{M}(\boldsymbol{x})\ddot{\boldsymbol{x}} + \boldsymbol{f_{in}}(\boldsymbol{x}, \dot{\boldsymbol{x}}) + \boldsymbol{C}\dot{\boldsymbol{x}} + \boldsymbol{f_{int}}(\boldsymbol{x}) = \boldsymbol{T}\cos(\omega t)$$

- One selects a control parameter, λ $\rightarrow$ ω, T, ...

Frequency approach

- Governing equations can be written in the following form

$$\boldsymbol{M}(\boldsymbol{x})\ddot{\boldsymbol{x}} + \boldsymbol{f_{in}}(\boldsymbol{x}, \dot{\boldsymbol{x}}) + \boldsymbol{C}\dot{\boldsymbol{x}} + \boldsymbol{f_{int}}(\boldsymbol{x}) = \boldsymbol{T}\cos(\omega t)$$

- One selects a control parameter, λ $\rightarrow$ $\omega,\ T,\ \dots$

- Unknows are expanded in a truncated Fourier series $\rightarrow$ Approximate Solutions
  - $\boldsymbol{x}(t) = \boldsymbol{x_0} + \sum_{i=1}^{H} \boldsymbol{x_{ci}}\cos(i\omega t) + \boldsymbol{x_{si}}\sin(i\omega t)$

Frequency approach

- Governing equations can be written in the following form

$$\boldsymbol{M}(\boldsymbol{x})\ddot{\boldsymbol{x}} + \boldsymbol{f_{in}}(\boldsymbol{x}, \dot{\boldsymbol{x}}) + \boldsymbol{C}\dot{\boldsymbol{x}} + \boldsymbol{f_{int}}(\boldsymbol{x}) = \boldsymbol{T}\cos(\omega t)$$

- One selects a control parameter, λ → ω, T, ...
- Unknows are expanded in a truncated Fourier series → Approximate Solutions
  - $\boldsymbol{x}(t) = \boldsymbol{x_0} + \sum_{i=1}^{H} \boldsymbol{x_{ci}} \cos(i\omega t) + \boldsymbol{x_{si}} \sin(i\omega t)$
- Harmonic Balance Method → Harmonics higher than H are neglected
  - The coefficient of each of the lowest $H+1$ harmonics are equated to zero

Frequency approach

- Governing equations can be written in the following form

$$\boldsymbol{M}(\boldsymbol{x})\ddot{\boldsymbol{x}} + \boldsymbol{f_{in}}(\boldsymbol{x}, \dot{\boldsymbol{x}}) + \boldsymbol{C}\dot{\boldsymbol{x}} + \boldsymbol{f_{int}}(\boldsymbol{x}) = \boldsymbol{T}\cos(\omega t)$$

- One selects a control parameter, λ → ω, T, ...

- Unknows are expanded in a truncated Fourier series → Approximate Solutions
  - $\boldsymbol{x}(t) = \boldsymbol{x_0} + \sum_{i=1}^{H} \boldsymbol{x_{ci}} \cos(i\omega t) + \boldsymbol{x_{si}} \sin(i\omega t)$

- Harmonic Balance Method → Harmonics higher than H are neglected
  - The coefficient of each of the lowest $H+1$ harmonics are equated to zero

- Non linear algebraic system resulting from HBM to solve → $\boldsymbol{U} = [\boldsymbol{x_0}\ \boldsymbol{x_{ci}}\ \boldsymbol{x_{si}}\ \dots\ \boldsymbol{x_{cH}}\ \boldsymbol{x_{sH}}]$
  - $\boldsymbol{R}(\boldsymbol{U}, \lambda) = 0$

Asymptotic Numerical Method (ANM)

Final system to solve can be written :

$$\boldsymbol{R}(\boldsymbol{U}, \lambda) = 0$$

Asymptotic Numerical Method (ANM)

Final system to solve can be written :

$$\boldsymbol{R}(\boldsymbol{U}, \lambda) = 0$$

- ANM is based on a high order perturbation method from an initial solution $(\boldsymbol{U_0}, \boldsymbol{\lambda_0})$

$$\boldsymbol{U}(a) = \boldsymbol{U_0} + a\boldsymbol{U_1} + a^2\boldsymbol{U_2} + ... + a^N\boldsymbol{U_N}$$
$$\lambda(a) = \lambda_0 + a\lambda_1 + a^2\lambda_2 + ... + a^N\lambda N$$

Asymptotic Numerical Method (ANM)

Final system to solve can be written :

$$\boldsymbol{R}(\boldsymbol{U}, \lambda) = 0$$

- ANM is based on a high order perturbation method from an initial solution $(\boldsymbol{U_0}, \boldsymbol{\lambda_0})$

$$\boldsymbol{U}(a) = \boldsymbol{U_0} + a\boldsymbol{U_1} + a^2\boldsymbol{U_2} + ... + a^N\boldsymbol{U_N}$$
$$\lambda(a) = \lambda_0 + a\lambda_1 + a^2\lambda_2 + ... + a^N\lambda N$$

- The solution is represented by a succession of local polynomial approximations as a function of a, the pseudo arc-length along the branch of solution

Asymptotic Numerical Method (ANM)

Final system to solve can be written :

$$\boldsymbol{R}(\boldsymbol{U}, \lambda) = 0$$

- ANM is based on a high order perturbation method from an initial solution $(\boldsymbol{U_0}, \boldsymbol{\lambda_0})$

$$\boldsymbol{U}(a) = \boldsymbol{U_0} + a\boldsymbol{U_1} + a^2\boldsymbol{U_2} + ... + a^N\boldsymbol{U_N}$$
$$\lambda(a) = \lambda_0 + a\lambda_1 + a^2\lambda_2 + ... + a^N\lambda N$$

- The solution is represented by a succession of local polynomial approximations as a function of a, the pseudo arc-length along the branch of solution
- piecewise continuous representation

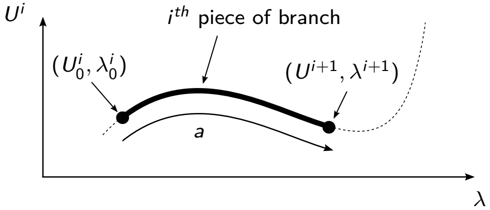

- The ANM becomes very efficient if $\boldsymbol{R}(\boldsymbol{U}, \lambda)$ is recasted in quadratic form

$$\boldsymbol{R}(\tilde{\boldsymbol{U}}) = \boldsymbol{C} + \boldsymbol{L}(\tilde{\boldsymbol{U}}) + \boldsymbol{Q}(\tilde{\boldsymbol{U}}, \tilde{\boldsymbol{U}}) = 0, \quad \tilde{\boldsymbol{U}} = [\boldsymbol{U}, \lambda]$$

MANLAB

- in practice, the software MANLAB 2.0 has been used to conpute the prediodic solutions. [Arquier 2007],[Cochelin & Vergez 2009]

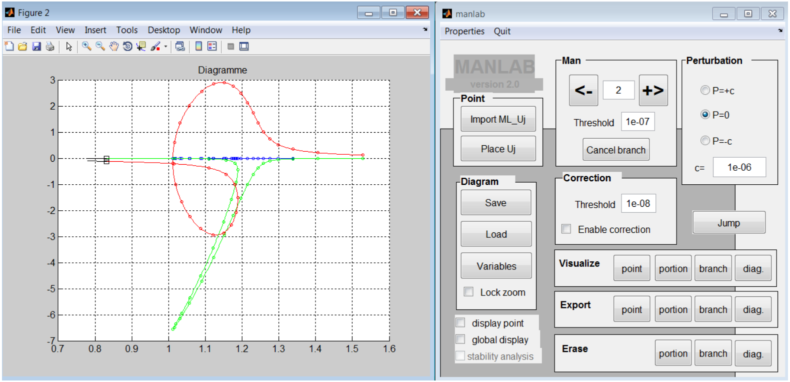

http ://manlab.lma.cnrs-mrs.fr/

Forced steady state response

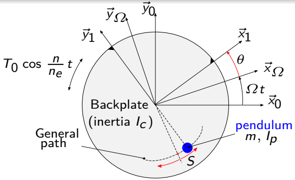

- The input order n is swept at constant torque amplitude
  - $\boldsymbol{x}(t) = \boldsymbol{x_0} + \sum_{i=1}^{H} \boldsymbol{x_{ci}} \cos(i \frac{n}{n_e} t) + \boldsymbol{x_{si}} \sin(i \frac{n}{n_e} t) \quad \boldsymbol{x} = [\theta, S]$
    - $H = 9$

Forced steady state response

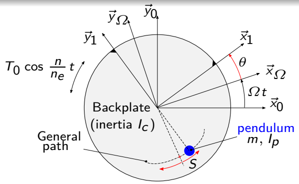

- The input order n is swept at constant torque amplitude
  - $x(t) = x_0 + \sum_{i=1}^{H} x_{ci} \cos(i \frac{n}{n_e} t) + x_{si} \sin(i \frac{n}{n_e} t) \quad x = [\theta, S]$
    - $H = 9$

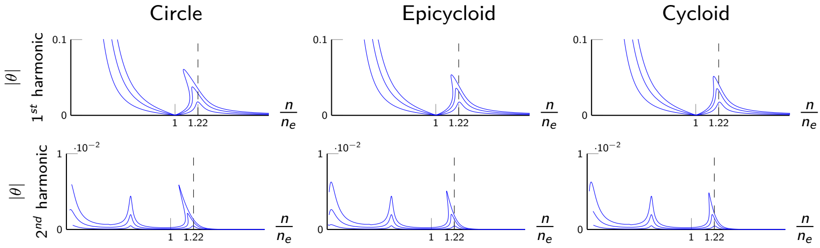

- Primary resonance exhibits softening behavior

Forced steady state response

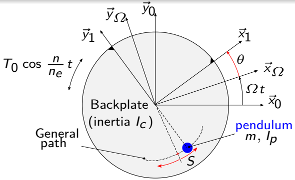

- The input order n is swept at constant torque amplitude
  - $x(t) = x_0 + \sum_{i=1}^{H} x_{ci} \cos(i \frac{n}{n_e} t) + x_{si} \sin(i \frac{n}{n_e} t) \quad x = [\theta, S]$
    - $H = 9$

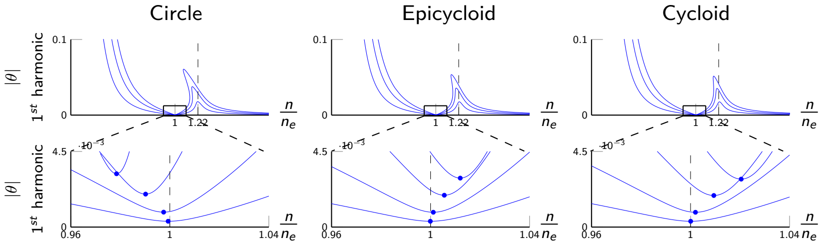

- Primary resonance exhibits softening behavior
- Loss of the tuning of the absorber at large amplitudes

Forced steady state response

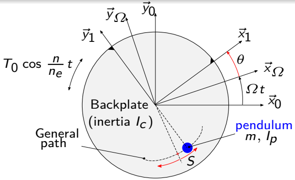

- The input order n is swept at constant torque amplitude
  - $x(t) = x_0 + \sum_{i=1}^{H} x_{ci} \cos(i \frac{n}{n_e} t) + x_{si} \sin(i \frac{n}{n_e} t) \quad x = [\theta, S]$
  - $H = 9$, $H = 1$

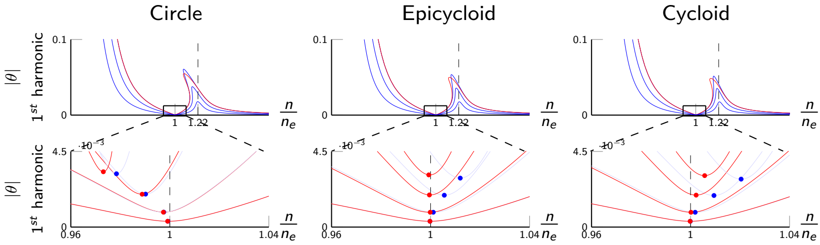

- Primary resonance exhibits softening behavior
- Loss of the tuning of the absorber at large amplitudes
- convergence as a function af the number of harmonic

Forced steady state response

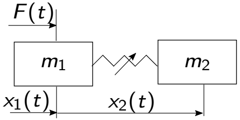

- No non linear inertial coupling

$$\begin{cases} \ddot{x}_1\left(m_1+m_2\right)+\ddot{x}_2 m_2=f\cos\omega t \\ \ddot{x}_1 m_2+\ddot{x}_2 m_2+k x_2+\gamma x_2^3=0 \end{cases}$$

Forced steady state response

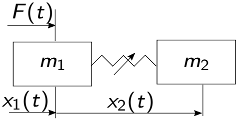

- No non linear inertial coupling

$$\begin{cases} \ddot{x}_1\,(m_1+m_2)+\ddot{x}_2\,m_2 = f\cos\omega t \\ \ddot{x}_1\,m_2+\ddot{x}_2\,m_2+kx_2+\gamma x_2^3 = 0 \end{cases}$$

$\gamma < 0$

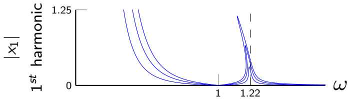

$\gamma > 0$

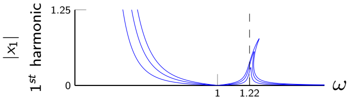

- The sign of γ governs the resonance behavior

Forced steady state response

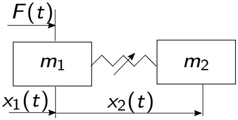

- No non linear inertial coupling

$$\begin{cases} \ddot{x}_1\,(m_1 + m_2) + \ddot{x}_2 m_2 = f \cos \omega t \\ \ddot{x}_1 m_2 + \ddot{x}_2 m_2 + k x_2 + \gamma x_2^3 = 0 \end{cases}$$

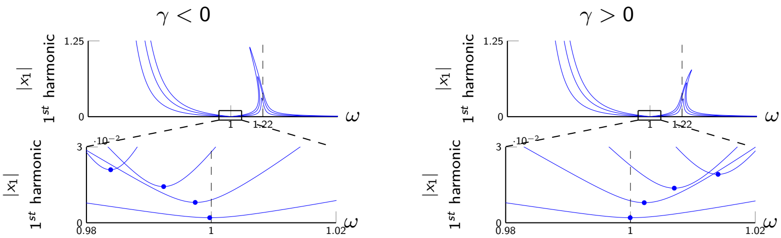

- The sign of γ governs the resonance behavior
- Antiresonance exhibits the same behavior as the resonance

Force continuation

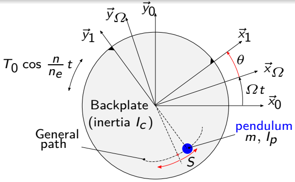

- The input torque amplitude T_0 is swept at constant excitation order $(n = n_e)$
  - $\boldsymbol{x}(t) = \boldsymbol{x_0} + \sum_{i=1}^{H} \boldsymbol{x_{ci}} \cos(i \frac{n}{n_e} t) + \boldsymbol{x_{si}} \sin(i \frac{n}{n_e} t) \quad \boldsymbol{x} = [\theta, S]$

Circular path

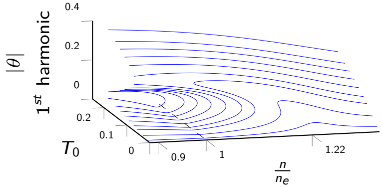

Force continuation

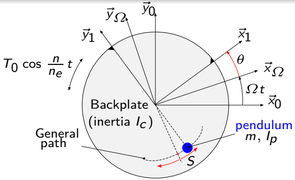

- The input torque amplitude T_0 is swept at constant excitation order $(n = n_e)$
  - $\boldsymbol{x}(t) = \boldsymbol{x_0} + \sum_{i=1}^{H} \boldsymbol{x_{ci}} \cos(i \frac{n}{n_e} t) + \boldsymbol{x_{si}} \sin(i \frac{n}{n_e} t) \quad \boldsymbol{x} = [\theta, S]$

Circular path

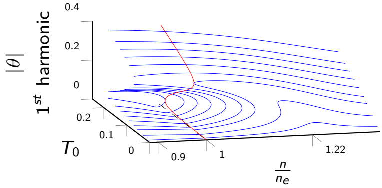

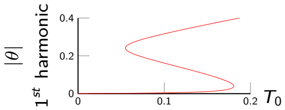

Force continuation

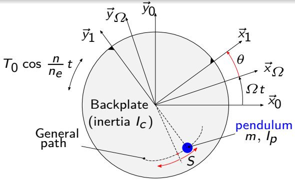

- The input torque amplitude T_0 is swept at constant excitation order $(n = n_e)$
  - $\boldsymbol{x}(t) = \boldsymbol{x_0} + \sum_{i=1}^{H} \boldsymbol{x_{ci}} \cos(i \frac{n}{n_e} t) + \boldsymbol{x_{si}} \sin(i \frac{n}{n_e} t) \quad \boldsymbol{x} = [\theta, S]$

Circular path

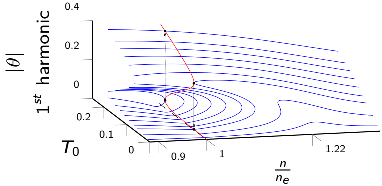

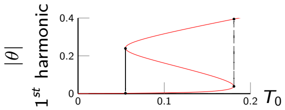

- Circular path absorbers exhibit strong jump phenomenon

Force continuation

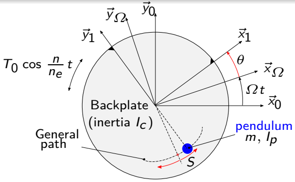

- The input torque amplitude T_0 is swept at constant excitation order ($n = n_e$)
  - $\boldsymbol{x}(t) = \boldsymbol{x_0} + \sum_{i=1}^{H} \boldsymbol{x_{ci}} \cos(i \frac{n}{n_e} t) + \boldsymbol{x_{si}} \sin(i \frac{n}{n_e} t) \quad \boldsymbol{x} = [\theta, S]$

Epicycloidal and cycloidal paths

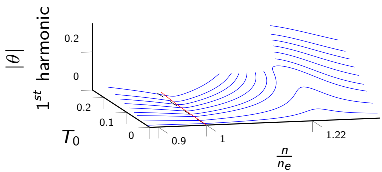

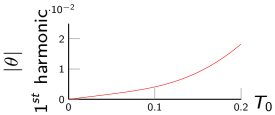

- Circular path absorbers exhibit strong jump phenomenon

Force continuation

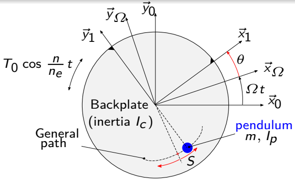

- The input torque amplitude T_0 is swept at constant excitation order $(n = n_e)$
  - $\boldsymbol{x}(t) = \boldsymbol{x_0} + \sum_{i=1}^{H} \boldsymbol{x_{ci}} \cos(i \frac{n}{n_e} t) + \boldsymbol{x_{si}} \sin(i \frac{n}{n_e} t) \quad \boldsymbol{x} = [\theta, S]$

Epicycloidal and cycloidal paths

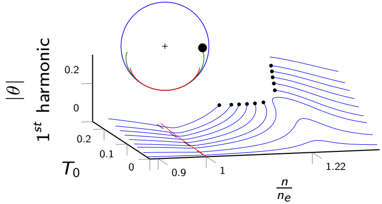

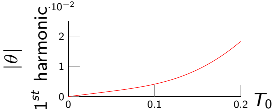

- Circular path absorbers exhibit strong jump phenomenon
- Epicycloid and cycloid path absorbers don't exhibit hysteretic jumps

Conclusion

- Use of continuation methods
  - No limitation in the number of harmonic
  - Epicycloid path is not tautochronic
- Hardening / softening behavior of the antiresonance highly depends on the path center of mass of the pendulum